

# Formation of an isolated wavefront dislocation

M. Ya. Darsht, B. Ya. Zel'dovich, I. V. Kataevskaya, and N. D. Kundikova

Technical University, 454080 Chelyabinsk, Russia

(Submitted 11 October 1994)

Zh. Éksp. Teor. Fiz. **107**, 1464–1472 (May 1995)

We proposed, studied theoretically, and realized experimentally the possibility of the formation of a wavefront with an isolated screw dislocation of a given sign during the passage of circularly polarized light through a multimode optical fiber. © 1995 American Institute of Physics.

## 1. INTRODUCTION

When scalar waves are scattered by stationary objects, singular points appear in the wavefront. These points are, in many respects, analogous to two-dimensional defects of a crystal lattice and they have the same name—dislocations.<sup>1,2</sup> Wavefront dislocations, as dislocations in a crystal, can be edge and screw dislocations as well as dislocations of a mixed type. Screw dislocations can be left-handed (negative) or right-handed (positive).<sup>1</sup> The possibility of the existence of wavefront dislocations was first demonstrated in Ref. 1, where solutions exhibiting the properties of dislocations were presented for the scalar wave equation. Dislocations can arise in ultrasonic waves<sup>3</sup> and in tidal waves in the ocean.<sup>4</sup> Wavefront dislocations in different nonoptical fields are studied in Refs. 5 and 6.

The possibility of dislocations in optical fields with speckle structure was first pointed out in Ref. 7. Such spatially nonuniform fields arise during the scattering of coherent light by a nonuniform surface and during the passage of radiation through a nonuniform phase screen<sup>8</sup> or a multimode optical fiber.<sup>9</sup> The intensity distribution in the speckle fields is granular, and screw dislocations exist at those points where the modulus of the complex amplitude vanishes, i.e., the imaginary and real parts vanish simultaneously. The surface of constant phase near a point of zero amplitude is a single-threaded screw surface (right- or left-handed). At the point of zero amplitude the phase is indeterminate, and it changes by  $2\pi$  for every circuit of the wavefront surface about zero. In Ref. 7 the properties of dislocations were investigated theoretically in detail, and it was shown that dislocations can appear and disappear only in pairs of opposite sign, i.e., trajectories of dislocations start and end at points where dislocations of opposite sign merge. Wavefront dislocations in a speckled laser wave were recorded experimentally in Ref. 10. The density of wavefront dislocations in speckled light fields was investigated experimentally in Ref. 11. In the light fields investigated, dislocations of opposite sign were observed in pairs, and the number of dislocations was approximately equal to the number of speckles.

Studies of the influence of dislocations on the nonlinear interactions of light raises the problem of the formation of light waves with isolated (solitary) wavefront dislocations of definite sign. Such light waves can be obtained by passing a plane wave through a computer-generated hologram.<sup>9,12</sup>

In the present paper we consider the possibility of the

formation of a wavefront with an isolated dislocation of given sign in a physical experiment without using computers.

## 2. PROPAGATION OF CIRCULARLY POLARIZED LIGHT THROUGH AN OPTICAL FIBER

Let light propagate in an axisymmetric optical fiber with a stepped index profile  $n(r)$ :

$$n(r) = \begin{cases} n_{co}, & r/\rho < 1, \\ n_{cl}, & r/\rho > 1. \end{cases} \quad (1)$$

Here,  $r = |\mathbf{r}|$ ,  $(x, y) = \mathbf{r}$  are the transverse coordinates,  $\rho$  is the radius of the core, and  $n_{co}$  and  $n_{cl}$  are the refractive indices of the core and cladding, respectively.

In the paraxial approximation, corresponding to the truncated wave equation, polarization does not affect diffraction. Because of the nonuniformity of the refractive index, the spatial structure and polarization of the field are coupled. The symmetry conditions<sup>13</sup> make it possible to write down four polarization modes in the following form for any orbital angular momentum  $m$  ( $m \geq 0$ ) and radial quantum number  $N$ :

$$\begin{aligned} \mathbf{e}_{m,N}^{(1)}(r, \varphi) &= [\cos(m\varphi)\mathbf{e}_x - \sin(m\varphi)\mathbf{e}_y]F_{m,N}(r), \\ \mathbf{e}_{m,N}^{(2)}(r, \varphi) &= [\cos(m\varphi)\mathbf{e}_x + \sin(m\varphi)\mathbf{e}_y]F_{m,N}(r), \\ \mathbf{e}_{m,N}^{(3)}(r, \varphi) &= [\sin(m\varphi)\mathbf{e}_x + \cos(m\varphi)\mathbf{e}_y]F_{m,N}(r), \\ \mathbf{e}_{m,N}^{(4)}(r, \varphi) &= [\sin(m\varphi)\mathbf{e}_x - \cos(m\varphi)\mathbf{e}_y]F_{m,N}(r). \end{aligned} \quad (2)$$

Here,  $\mathbf{e}_x$  and  $\mathbf{e}_y$  are unit vectors,  $x = r\cos\varphi$ , and  $y = r\sin\varphi$ . The radial function  $F_{m,N}(r)$  has the form

$$F_{m,N}(r) = \begin{cases} J_m(U_N r), & r/\rho < 1, \\ K_m(W_N r), & r/\rho > 1. \end{cases} \quad (3)$$

Here,  $J_m$  and  $K_m$  are Bessel functions, and the quantities  $U_N$  and  $W_N$  are determined for each value of  $m$  from the equation

$$U_N \frac{J_{m+1}(U_N)}{J_m(U_N)} = W_N \frac{K_{m+1}(W_N)}{K_m(W_N)}, \quad (4)$$

$V^2 = W_N^2 + U_N^2$ ,  $V = \rho k \sqrt{2n_{co}(n_{co} - n_{cl})}$ ,  $k = 2\pi/\lambda$ , and  $\lambda$  is the wavelength of light in air.

If the orbital angular momentum  $m$  takes on the values 0 and 1, then the polarization corrections  $\delta\beta_{m,N}^{(j)}$  to the propagation constant  $\beta_{m,N}$  are<sup>13</sup>

$$\begin{aligned} \delta\beta_{0,N}^{(1)} &= \delta\beta_{0,N}^{(3)} = \delta\beta_{0,N}^{(2)} = \delta\beta_{0,N}^{(4)} \\ &= -\frac{(2\Delta)^{3/2} W_N U_N^2 K_0(W_N)}{2\rho V^3 K_1(W_N)}, \end{aligned} \quad (5)$$

$$\delta\beta_{1,N}^{(1)} = \delta\beta_{1,N}^{(3)} = -\frac{(2\Delta)^{3/2} W_N U_N^2 K_1(W_N)}{2\rho V^3 K_0(W_N)}, \quad (6)$$

$$\delta\beta_{1,N}^{(2)} = \frac{(2\Delta)^{3/2} W_N U_N^2 K_1(W_N)}{\rho V^3 K_2(W_N)}, \quad (7)$$

$$\delta\beta_{1,N}^{(4)} = 0, \quad (8)$$

and  $\Delta \approx (n_{co} - n_{cl})/n_{cl}$ .

For values of the orbital angular momentum  $m > 1$ , the polarization corrections  $\delta\beta_{m,N}^{(j)}$  acquire the following form:<sup>13</sup>

$$\delta\beta_{m,N}^{(1)} = \delta\beta_{m,N}^{(3)} = \frac{(2\Delta)^{3/2} W_N U_N^2 K_m(W_N)}{2\rho V^3 K_{m-1}(W_N)}, \quad (9)$$

$$\delta\beta_{m,N}^{(2)} = \delta\beta_{m,N}^{(4)} = \frac{(2\Delta)^{3/2} W_N U_N^2 K_m(W_N)}{2\rho V^3 K_{m+1}(W_N)}. \quad (10)$$

Any linear combinations of the modes  $\mathbf{e}_{m,N}^{(1)}$  and  $\mathbf{e}_{m,N}^{(3)}$  for all values of  $m$  and any linear combinations of the modes  $\mathbf{e}_{m,N}^{(2)}$  and  $\mathbf{e}_{m,N}^{(4)}$  in the case  $m \neq 1$  will also be eigenmodes. It is easy to show that the combinations  $\mathbf{e}_{m,N}^{(1)} \pm i\mathbf{e}_{m,N}^{(3)}$  and  $\mathbf{e}_{m,N}^{(2)} \pm i\mathbf{e}_{m,N}^{(4)}$  are modes with constant circular polarization  $\mathbf{e}_x + i\sigma\mathbf{e}_y$  throughout the fiber. Here  $\sigma = 1$  for light with right-hand circular polarization and  $\sigma = -1$  for light with left-hand circular polarization. These new modes are:

$$\begin{aligned} \mathbf{e}_{+,m,N}^+(r, \varphi) &= \mathbf{e}_{m,N}^{(1)}(r, \varphi) + i\mathbf{e}_{m,N}^{(3)}(r, \varphi) = (\mathbf{e}_x + i\mathbf{e}_y) \\ &\quad \times e^{im\varphi} F_{m,N}(r), \\ \mathbf{e}_{-,m,N}^-(r, \varphi) &= \mathbf{e}_{m,N}^{(1)}(r, \varphi) - i\mathbf{e}_{m,N}^{(3)}(r, \varphi) = (\mathbf{e}_x - i\mathbf{e}_y) \\ &\quad \times e^{-im\varphi} F_{m,N}(r), \\ \mathbf{e}_{+,m,N}^-(r, \varphi) &= \mathbf{e}_{m,N}^{(2)}(r, \varphi) + i\mathbf{e}_{m,N}^{(4)}(r, \varphi) = (\mathbf{e}_x - i\mathbf{e}_y) \\ &\quad \times e^{im\varphi} F_{m,N}(r), \\ \mathbf{e}_{-,m,N}^+(r, \varphi) &= \mathbf{e}_{m,N}^{(2)}(r, \varphi) - i\mathbf{e}_{m,N}^{(4)}(r, \varphi) = (\mathbf{e}_x + i\mathbf{e}_y) \\ &\quad \times e^{-im\varphi} F_{m,N}(r). \end{aligned} \quad (11)$$

Let a circularly polarized wave, with  $\sigma = 1$ , for example, enter the fiber:

$$\begin{aligned} \mathbf{E}^+(r, \varphi, z=0) &= (\mathbf{e}_x + i\mathbf{e}_y) \left[ e^{-i\varphi} \sum_N C_{-,1,N} F_{1,N}(r) \right. \\ &\quad + \sum_{m \neq 1} \sum_N C_{-,m,N} e^{-im\varphi} F_{m,N}(r) \\ &\quad \left. + \sum_m \sum_N C_{+,m,N} e^{im\varphi} F_{m,N}(r) \right]. \end{aligned} \quad (12)$$

Here, the coefficients  $C_{+,m,N}$  and  $C_{-,m,N}$  determine the contribution of the modes  $\mathbf{e}_{+,m,N}^+(r, \varphi)$  and  $\mathbf{e}_{-,m,N}^-(r, \varphi)$  to the light field at the fiber entrance. The distribution of the field at the fiber exit is

$$\begin{aligned} \mathbf{E}^+(r, \varphi, z) &= (\mathbf{e}_x + i\mathbf{e}_y) \\ &\quad \times \left\{ \sum_{m \neq 1} \sum_N C_{-,m,N} e^{-im\varphi} F_{m,N}(r) \exp[iz(\beta_{m,N} \right. \\ &\quad \left. + \delta\beta_{m,N}^{(2)})] \right. \\ &\quad + \sum_m \sum_N C_{+,m,N} e^{im\varphi} F_{m,N}(r) \exp[iz(\beta_{m,N} \\ &\quad \left. + \delta\beta_{m,N}^{(1)})] \right. \\ &\quad \left. + \sum_N C_{-,1,N} e^{-i\varphi} F_{1,N}(r) e^{iz\beta_{1,N}} (e^{i2z\delta\beta_{1,N}^{(2)}} + 1) \right\} \\ &\quad + (\mathbf{e}_x - i\mathbf{e}_y) \\ &\quad \times \left[ e^{i\varphi} \sum_N C_{-,1,N} F_{1,N}(r) e^{iz\beta_{1,N}} (e^{i2z\delta\beta_{1,N}^{(2)}} - 1) \right]. \end{aligned} \quad (13)$$

A similar expression can be obtained when circularly polarized radiation with  $\sigma = -1$  enters the fiber:

$$\begin{aligned} \mathbf{E}^-(r, \varphi, z) &= (\mathbf{e}_x - i\mathbf{e}_y) \\ &\quad \times \left\{ \sum_{m \neq 1} \sum_N C_{+,m,N} e^{im\varphi} F_{m,N}(r) \exp[iz(\beta_{m,N} \right. \\ &\quad \left. + \delta\beta_{m,N}^{(2)})] + \sum_m \sum_N C_{-,m,N} e^{-im\varphi} F_{m,N}(r) \right. \\ &\quad \left. \times \exp[iz(\beta_{m,N} + \delta\beta_{m,N}^{(1)})] + \sum_N C_{+,1,N} \right. \\ &\quad \left. \times e^{i\varphi} F_{1,N}(r) e^{iz\beta_{1,N}} (e^{i2z\delta\beta_{1,N}^{(2)}} + 1) \right\} + (\mathbf{e}_x + i\mathbf{e}_y) \\ &\quad \times \left[ e^{-i\varphi} \sum_N C_{+,1,N} F_{1,N}(r) e^{iz\beta_{1,N}} (e^{i2z\delta\beta_{1,N}^{(2)}} - 1) \right]. \end{aligned} \quad (14)$$

It follows from (13) and (14) that when circularly polarized light propagates in a multimode fiber, only the  $\mathbf{e}_{1,N}^2$  and  $\mathbf{e}_{1,N}^4$  modes contribute to the "foreign" polarization. The  $\mathbf{e}_{1,N}^2$  and  $\mathbf{e}_{1,N}^4$  modes are indeed special modes, since in the geometrical optics interpretation they correspond to meridional rays for which circular polarization is not conserved because of symmetry considerations.<sup>13,14</sup>

If a "circular analyzer" that transmits circular radiation opposite in sign to  $\sigma$  at the fiber entrance is placed at the fiber exit, it will pass only the corresponding modes with  $m = 1$ . We shall study in greater detail the field passing through the "circular analyzer." This field is described by the last term in the sums (13) and (14). If light with  $\sigma = 1$  enters the fiber the field  $E^{+-}$  that passes through the "circular analyzer" has the following form:

$$E^{+-} = e^{i\varphi} \left\{ \sum_N C_{-1,N} F_{1,N}(r) \exp(iz\beta_{1,N}) \times [\exp(i2z\delta\beta_{1,N}^{(2)}) - 1] \right\}. \quad (15)$$

The factor  $e^{i\varphi}$  indicates that the wavefront of the field (15) contains one positive screw dislocation.

If the entrance to the waveguide is illuminated with circularly polarized radiation with  $\sigma = -1$  and circularly polarized radiation with  $\sigma = +1$  is extracted at the waveguide exit, the field  $E^{-+}$  after the "circular analyzer" will have the form

$$E^{-+} = e^{-i\varphi} \left\{ \sum_N C_{+1,N} F_{1,N}(r) \exp(iz\beta_{1,N}) \times [\exp(i2z\delta\beta_{1,N}^{(2)}) - 1] \right\}, \quad (16)$$

i.e., the light field (16) will contain a left-handed screw dislocation.

It follows from (15) and (16) that the distribution of the intensity  $I^{+-} = E^{+-} \cdot (E^{+-})^*$  across the fiber does not depend on  $\varphi$ , i.e., it is axisymmetric. In the special case of an optical fiber with a small number of modes, such that  $N_{\max} = 1$  for  $m = 1$ , the intensity of the "foreign" polarization is a periodic function of the fiber length:

$$I^{+-} = [C_{-1,1} F_{1,1}(r)]^2 [1 - \cos(2z\delta\beta_{1,1}^{(2)})]. \quad (17)$$

The intensity  $I^{+-}$  is maximum for fiber lengths

$$z_n = \frac{\pi(2n+1)}{2\delta\beta_{1,1}^{(2)}}. \quad (18)$$

Therefore, if circularly polarized radiation with a definite sign of  $\sigma$  is fed to a multimode fiber with a stepped index profile and circularly polarized radiation of the opposite sign is extracted at the output the transmitted radiation will consist of a light wave with an isolated wavefront dislocation, and a sign change in  $\sigma$  at the fiber input together with a corresponding sign change in the "circular analyzer" will result in a change in the sign of the screw dislocation.

All arguments presented above are also valid if separate modes do not interact with one another when light propagates through an optical fiber. This assertion is certainly applicable to the propagation of  $\sim 5$  mW He-Ne-laser light in a quartz fiber.<sup>13</sup> The validity of this approximation was also demonstrated in Ref. 15, where very good quantitative agreement was obtained between the computed and experimentally measured angle of rotation of the speckle pattern in observations of the optical analog of the Magnus effect.

We now consider what the interference pattern of a reference plane wave and a converging wave with a positive or negative unit screw wavefront dislocation looks like on a screen. Figure 1a displays the computed lines of maximum intensity of the interference pattern on a screen in the case of a plane wave and a converging wave  $\mathbf{E} \sim \mathbf{A}(\mathbf{r}, z, t) e^{i\varphi}$  with a positive dislocation, and Fig. 1b displays the computed lines of maximum intensity of the interference pattern obtained

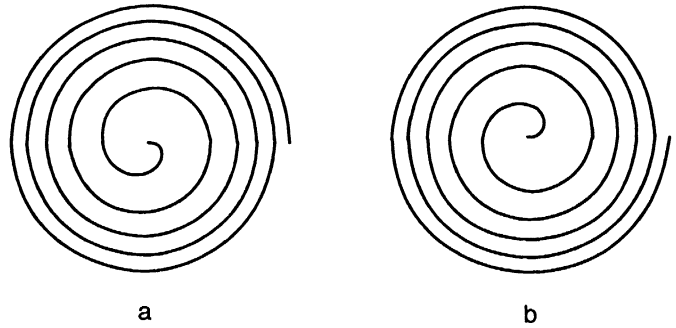


FIG. 1. Curves of maximum intensity in the interference pattern formed by a plane wave and converging waves: a— $\mathbf{E} \sim \mathbf{A}(\mathbf{r}, z, t) e^{i\varphi}$ ; b— $\mathbf{E} \sim \mathbf{A}(\mathbf{r}, z, t) e^{-i\varphi}$ .

with a plane wave and a converging wave  $\mathbf{E} \sim \mathbf{A}(\mathbf{r}, z, t) e^{-i\varphi}$  with a negative dislocation. As one can see from the figure, the interference pattern is a spiral which unwinds in the clockwise direction in the case of a positive screw dislocation and in the counterclockwise direction if the wave contains a single negative screw dislocation. It follows from Fig. 1 that when the sign of the screw dislocation changes, so does the direction in which the spiral unwinds. This means, in turn, that when the sign of the circular polarization at the input and output changes, the direction in which the spiral unwinds should also change.

### 3. FORMATION OF A WAVEFRONT WITH AN ISOLATED DISLOCATION

To produce a light wave experimentally whose wavefront contains an isolated dislocation, we chose an optical fiber with a stepped index profile and the following parameters: fiber core diameter  $2\rho = 9 \mu\text{m}$ , difference between the index of refraction of the core and cladding  $\Delta n = n_{\text{co}} - n_{\text{cl}} = 0.004$ .

The solution of Eq. (4) for a fiber with such parameters gives the values  $m = 0, 1, 2$ . The quantity  $N = 1, 2$  for  $m = 0$  and  $N = 1$  for  $m = 1, 2$ . Therefore, twelve modes can propagate in the fiber:

$$\begin{aligned} M_1 &= \mathbf{e}_{0,1}^{(1)}(r, \varphi), & M_2 &= \mathbf{e}_{0,1}^{(3)}(r, \varphi), & M_3 &= \mathbf{e}_{0,2}^{(1)}(r, \varphi), \\ M_4 &= \mathbf{e}_{0,2}^{(3)}(r, \varphi), & M_5 &= \mathbf{e}_{1,1}^{(1)}(r, \varphi), & M_6 &= \mathbf{e}_{1,1}^{(2)}(r, \varphi), \\ M_7 &= \mathbf{e}_{1,1}^{(3)}(r, \varphi), & M_8 &= \mathbf{e}_{1,1}^{(4)}(r, \varphi), & M_9 &= \mathbf{e}_{2,1}^{(1)}(r, \varphi), \\ M_{10} &= \mathbf{e}_{2,1}^{(2)}(r, \varphi), & M_{11} &= \mathbf{e}_{2,1}^{(3)}(r, \varphi), & M_{12} &= \mathbf{e}_{2,1}^{(4)}(r, \varphi). \end{aligned} \quad (19)$$

Since  $N_{\max} = 1$  in the experimental fiber with  $m = 1$ , the optimum fiber length can be determined in accordance with (18). The polarization correction  $\delta\beta_{1,1}^{(2)}$ , determined from the expression (7), was found to be  $0.20526 \text{ cm}^{-1}$ . The chosen fiber length  $z_n$  corresponded to  $n = 7$  and was approximately 114 cm. This length also made it possible to work essentially independently with either end of the fiber.

A Mach-Zender interferometer scheme was used to record the wavefront with an isolated dislocation.

The experimental setup is shown in Fig. 2. The linearly polarized radiation from He-Ne-laser  $I$  with wavelength

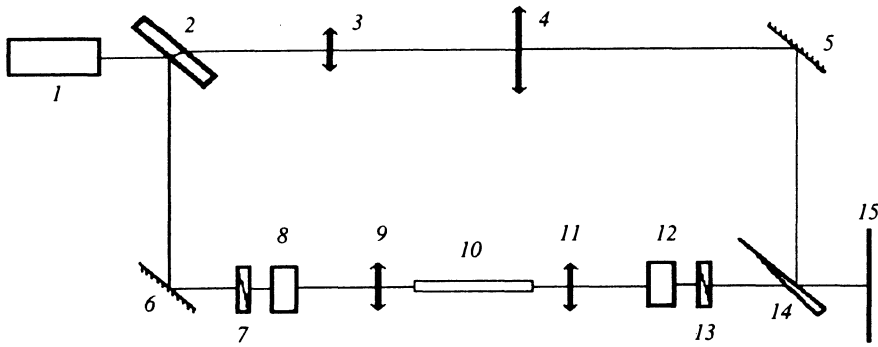


FIG. 2. Optical layout: 1—He-Ne-laser; 2—beam splitter; 3—objective; 4, 9, 11—lenses; 5, 6—mirrors; 7, 13—polarizers; 8, 12—quarter-wave plates; 10—fiber; 14—wedge; 15—screen.

$\lambda = 0.63 \mu\text{m}$  was divided into two beams  $J_0$  and  $J_c$  by beam-splitter 2. The beam  $J_0$  passed through a telescopic system consisting of an objective 3 and lens 4. The telescopic system expanded the beam diameters to 2.5 cm.

The beam  $J_c$  passed through polarizer 7 and quarter-wave plate 8. We emphasize that a tunable polarization device<sup>16</sup> that could be tuned to the required wavelength immediately prior to and in the course of the experiment was used as the quarter-wave plate. The device employed in this experiment<sup>16</sup> provided up to 98% circular polarization. The circularly polarized light ( $\sigma = 1$  or  $\sigma = -1$ ) was focused by lens 9 onto the fiber input 10. The radiation transmitted through the fiber consisted of a speckle pattern. The lens 11 made it possible to change the divergence of the speckle pattern at the fiber output and the speckle pattern was then transmitted through a wide-aperture “circular analyzer.” This analyzer consisted of a tunable quarter-wave plate 12 (Ref. 16) and a polarizer 13, and made it possible to separate circularly polarized radiation with  $\sigma = -1$  or  $\sigma = 1$ . In accordance with the results (17), the intensity distributions  $I^{+-}$  and  $I^{-+}$  must have the form of a uniform ring, but in reality the speckle pattern is only reminiscent of a ring, in which several nonuniformly illuminated regions could be identified. The interference of the beams  $J_0$  and  $J_c$  was observed on the screen 15.

Figure 3 shows photographs of the interference pattern on the screen 15 for the case in which the beam  $J_0$  is essentially parallel and the beam  $J_c$  is converging. Figure 3a corresponds to the situation in which circularly polarized light with  $\sigma = 1$  is incident on the fiber and a circularly polarized light wave with  $\sigma = -1$ , containing a positive screw wave-

front dislocation, is isolated by the “circular analyzer.” As one can see from the figure, the interference pattern is a clockwise spiral. Comparing with Fig. 1a shows that this result agrees completely with theory. Figure 3b displays a photograph of the interference pattern obtained when a plane wave and a wave with a negative wavefront dislocation formed when circularly polarized light with  $\sigma = -1$  passes through the fiber and the crossed “circular analyzer” interfere with one another. The interference pattern is a spiral which, like the spiral in Fig. 1b, unwinds in the counterclockwise direction. Therefore, this result also agrees completely with the expected result. We emphasize that only one spiral is observed in the interference pattern in Figs. 3a and 3b; this corresponds to an isolated wavefront dislocation. To check whether or not the dislocation is indeed the only dislocation, the wavefronts  $J_0$  and  $J_c$  were smoothed, and only one “extra” fringe was observed in the interference pattern.

Comparing Figs. 1 and 3 shows that the observed interference patterns correspond to the result expected from (15) and (16).

#### 4. CONCLUSIONS

As a result of this work, the possibility of the formation of a light wave with an isolated wavefront dislocation having a fixed sign was proposed and studied theoretically. Such a wave is formed when circularly polarized radiation passes through a multimode fiber-optic waveguide. The proposed scheme was realized experimentally. The result of the interference of a reference plane wave and the waves passing through a multimode optical fiber between crossed “circular

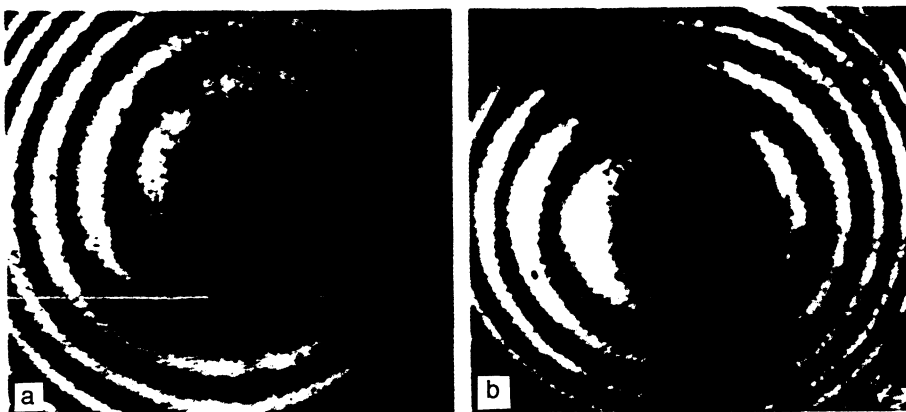


FIG. 3. Photographs of the interference pattern on the screen. a—Circularly polarized radiation with  $\sigma = 1$  incident at fiber input and circularly polarized radiation with  $\sigma = -1$  extracted from fiber output. b—Circularly polarized radiation with  $\sigma = -1$  incident at fiber input and circularly polarized radiation with  $\sigma = 1$  extracted from fiber output.

polarizers" showed that such waves have a single positive or negative wavefront dislocation. It was demonstrated that the sign of the dislocation changes when the sign of the "circular polarizers" at the entrance and exit from the waveguide changes. The experimental results agree with the theoretical predictions.

- <sup>1</sup>J. F. Nye and M. V. Berry, Proc. R. Soc. London A **336**, 165 (1974).
- <sup>2</sup>J. F. Nye, Proc. R. Soc. London A **378**, 219 (1981).
- <sup>3</sup>V. F. Humphrey, "Experimental observation of wavefront dislocations in pulsed wavefields," Ph.D. Thesis, University of Bristol (1980).
- <sup>4</sup>M. V. Berry, "Singularities in waves and rays" in *Les Houches Lecture Notes for Session 35*, R. Balian, M. Kleman, and J. P. Poirier, North-Holland, Amsterdam, 1981, p. 453.
- <sup>5</sup>F. J. Wright, "Wavefield singularities," Ph.D. Thesis, University of Bristol (1977).
- <sup>6</sup>M. V. Berry, J. Phys. A **11**, 27 (1978).
- <sup>7</sup>N. B. Baranova and B. Ya. Zel'dovich, Zh. Éksp. Teor. Fiz. **80**, 1780 (1981) [Sov. Phys. JETP **53**, 925 (1981)].
- <sup>8</sup>B. Ya. Zel'dovich, N. F. Pilipetskiĭ, and V. V. Shkunov, *Principles of*

*Phase Conjugation*, Springer-Verlag, New York, (1986).

- <sup>9</sup>V. Yu. Bazhenov, M. V. Vasnetsov, and M. S. Soskin, Pis'ma Zh. Éksp. Teor. Fiz. **52**, 1037 (1990) [JETP Lett. **52**, 429 (1990)].
- <sup>10</sup>N. B. Baranova, B. Ya. Zel'dovich, A. V. Mamaev, N. F. Pilipetskiĭ, and V. V. Shkunov, Pis'ma Zh. Éksp. Teor. Fiz. **33**, 206 (1981) [JETP Lett. **33**, 195 (1981)].
- <sup>11</sup>N. B. Baranova, B. Ya. Zel'dovich, A. V. Mamaev, N. F. Pilipetskiĭ, and V. V. Shkunov, Zh. Éksp. Teor. Fiz. **83**, 1702 (1982) [Sov. Phys. JETP **56**, 983 (1982)].
- <sup>12</sup>Yu. Bazhenov, M. S. Soskin, and M. V. Vasnetsov, J. Modern Optics **39**, 985 (1992).
- <sup>13</sup>A. W. Snyder and J. D. Love, *Optical Waveguide Theory*, Chapman and Hall, New York (1983).
- <sup>14</sup>N. B. Baranova and B. Ya. Zel'dovich, Pis'ma Zh. Éksp. Teor. Fiz. **59**, 648 (1994) [JETP Lett. **59**, 681 (1994)].
- <sup>15</sup>A. V. Dooghin, N. D. Kundikova, V. S. Liberman, and B. Ya. Zel'dovich, Phys. Rev. A **45**, 8204 (1992).
- <sup>16</sup>I. V. Gol'tser, M. Ya. Darsht, B. Ya. Zel'dovich, and N. D. Kundikova, Kvant. Élektron. **20**, 916 (1993) [Quantum Electron. **20**, 796 (1993)].

Translated by M. E. Alferieff